

Data-Driven Optimal ILC for Multivariable Systems: Removing the Need for L and Q Filter Design

Joost Bolder and Tom Oomen

Abstract—Many iterative learning control algorithms rely on a model of the system. Although only approximate model knowledge is required, the model quality determines the convergence and performance properties of the learning control algorithm. The aim of this paper is to remove the need for a model for a class of multivariable ILC algorithms. The main idea is to replace the model by dedicated experiments on the system. Convergence criteria are developed and the results are illustrated with a simulation on a multi-axis flatbed printer.

I. INTRODUCTION

Iterative learning control (ILC) [1] can significantly enhance the performance of systems that perform repeated tasks. After each repetition the command signal for the next repetition is updated by learning from past executions. Examples applications include: additive manufacturing machines [2], [3], robotic arms [4], printing systems [5], pick and place machines, electron microscopes, and wafer stages [6]–[8].

Iterative learning control algorithms such as frequency domain ILC [9], [10] and Optimal ILC [11]–[16] are to some extent model-based. The convergence and performance properties of these learning control algorithms hinge on a model of the controlled system. In particular, robustness to modeling errors is a key issue, as is evidenced by the development of robust ILC approaches such as [17]–[20].

Although there are substantial developments in robust ILC, such approaches drastically increase the modeling requirements. In particular, these approaches require both a nominal model and a description of model uncertainty. Especially in the multivariable situation, such models are difficult and expensive to obtain. The aim of this paper is to develop an optimal ILC algorithm for multivariable systems without the need of a model to design L and Q filters. In fact, the proposed approach will have no L and Q filters in the usual ILC sense.

The main difficulty in the development of the presented approach lies in the multivariable aspect. When the proposed approach is applied to the special case of single-input single-output systems, a well-known result is recovered that is closely related to the commonly used “FiltFilt” approach in Q -filtering [21, Section 36.3.3.1]. This standard solution is also well-known and commonly applied in system identification [22], [23], [24, Section 12.2], as well as in ILC [25]–[29]. The main contribution of this paper lies in a fully data-driven optimal ILC approach for *multivariable* systems.

The authors are with the Eindhoven University of Technology, Dept. of Mechanical Engineering, Control Systems Technology group, P.O. Box 513, 5600 MB Eindhoven, The Netherlands, j.j.bolder@tue.nl

This is achieved by exploiting recent results in the system identification approach in [30].

The outline of this paper is as follows. In the next section, the problem is stated and the contributions are summarized. Then, in Section III, the data-based ILC algorithm is developed and convergence criteria are provided. The results are supported with a simulation example using the model of an industrial multi-axis flatbed printer in Section IV. Finally, the conclusions and ongoing research topics are presented in Section V.

II. PROBLEM DEFINITION AND CONTRIBUTIONS

Many important ILC algorithms hinge on a model of the controlled system. Due to the increased modeling complexity in robust ILC approaches for multivariable systems, it is especially relevant that data-driven ILC algorithms possess inherent robustness against modeling errors, see [31] for a survey.

Therefore, the aim of this paper is to present an optimal ILC algorithm for multivariable systems that does not require to design L and Q filters. An approach for multivariable point-to-point problems is presented in [32]. The results in the present paper are applicable to both point-to-point as well as tracking problems. The main contributions are as follows:

- 1) the development of a data-driven adjoint-based ILC algorithm including analysis of the convergence aspects, see Section III,
- 2) the results are illustrated in a simulation on a multi-axis industrial flatbed printer, see Section IV.

III. DATA-DRIVEN LEARNING: ADJOINT-BASED ILC

This section constitutes contribution 1, see Section II.

A. Preliminaries

A matrix $B \in \mathbb{R}^{N \times N}$ is defined positive (semi-)definite iff $x^T B x \geq 0, \forall x \neq 0, x \in \mathbb{R}^N$ and is denoted as $B \geq 0$. For a vector x , $\|x\|_W = x^T W x$. Consider a single-input single-output (SISO) system J^{11} with transfer function:

$$J^{11}(z) = \sum_{i=0}^{\infty} h_i z^{-i},$$

here $h_i \in \mathbb{R}$, $i = 0, \dots, \infty(z)$ are the Markov parameters of J^{11} , and $z \in \mathbb{C}$. It is assumed that signals have finite length $N \in \mathbb{N}$. The response of the system $y^1 = J^{11}u^1$ for the finite-time interval $0 \leq k < N$ is denoted as:

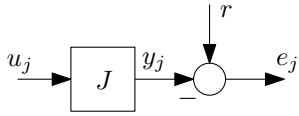


Fig. 1. Multivariable ILC setup.

$$\underbrace{\begin{bmatrix} y^1(0) \\ y^1(1) \\ \vdots \\ y^1(N-1) \end{bmatrix}}_{y^1} = \underbrace{\begin{bmatrix} h(0) & 0 & \dots & 0 \\ h(1) & \ddots & \ddots & \vdots \\ \vdots & \ddots & \ddots & 0 \\ h(N-1) & \dots & h(1) & h(0) \end{bmatrix}}_{J^{11}} \underbrace{\begin{bmatrix} u^1(0) \\ u^1(1) \\ \vdots \\ u^1(N-1) \end{bmatrix}}_{u^1}, \quad (1)$$

with $y^1 \in \mathbb{R}^N$, $u^1 \in \mathbb{R}^N$, and $J^{11} \in \mathbb{R}^{N \times N}$ a matrix representation of $\mathbf{J}^{11}(z)$.

Consider a multiple-input multiple-output (MIMO) system J with transfer function matrix $\mathbf{J}(z) \in \mathbb{C}^{n_o \times n_i}$, with n_i the number of inputs, n_o the number of outputs. The finite-time response for the MIMO system J is denoted as

$$\underbrace{\begin{bmatrix} y^1 \\ \vdots \\ y^{n_o} \end{bmatrix}}_y = \underbrace{\begin{bmatrix} J^{11} & \dots & J^{1,n_i} \\ \vdots & & \vdots \\ J^{n_o,1} & \dots & J^{n_o,n_i} \end{bmatrix}}_J \underbrace{\begin{bmatrix} u^1 \\ \vdots \\ u^{n_i} \end{bmatrix}}_u, \quad (2)$$

where J^{ij} the matrix representation of the i th entry in $\mathbf{J}(z)$, $y^i \in \mathbb{R}^N$, $u^i \in \mathbb{R}^N$, $y \in \mathbb{R}^{n_o N}$, $u \in \mathbb{R}^{n_i N}$, and $J \in \mathbb{R}^{n_o N \times n_i N}$ is the matrix representation of $\mathbf{J}(z)$.

B. Optimal adjoint-based ILC

The ILC framework used in this paper is presented in Fig. 1. The system $J \in \mathbb{R}^{n_o N \times n_i N}$ is a MIMO system with output $y_j \in \mathbb{R}^{n_o N}$, input $u_j \in \mathbb{R}^{n_i N}$ and reference $r \in \mathbb{R}^{n_o N}$. The trial index is denoted as j . From Fig. 1 follows the tracking error

$$e_j = r - Ju_j.$$

The error propagation from trial j to $j+1$ is given by

$$e_{j+1} = e_j - J(u_{j+1} - u_j), \quad (3)$$

and follows by eliminating r from $e_{j+1} = r - Ju_{j+1}$.

Optimal ILC is an important class of ILC algorithms, e.g., [14]–[16], where u_{j+1} is determined by minimizing a cost function. The optimization criterion used in this paper is defined as follows.

Definition 1 (Performance criterion). *The performance $\mathcal{J}(u_{j+1})$ is given by*

$$\mathcal{J}(u_{j+1}) := \|e_{j+1}\|_{W_e} + \|u_{j+1}\|_{W_f}, \quad (4)$$

with $\|x\|_W = x^T W x$, $W_e \in \mathbb{R}^{n_o N \times n_o N}$, $W_f \in \mathbb{R}^{n_o N \times n_o N}$.

In Definition 1, $W_e > 0$, $W_f \geq 0$ are weight matrices. The following theorem presents a gradient-descent ILC algorithm for minimizing (4). For similar lines as followed here, see e.g., [14]–[16], [25], and [26].

Theorem 2 (Gradient descent ILC algorithm). *The gradient descent (or steepest descent) ILC algorithm that minimizes (4) is given by*

$$u_{j+1} = (I - \varepsilon W_f)u_j + \varepsilon J^T W_e e_j, \quad (5)$$

with $0 < \varepsilon \leq \bar{\varepsilon}$ the learning gain.

Proof. The gradient of (4) at the current ILC command signal u_j is given by

$$\left. \frac{\partial \mathcal{J}(u_{j+1})}{\partial u_{j+1}} \right|_{u_{j+1}=u_j} = -2J^T W_e e_j + 2W_f u_j.$$

The gradient descent algorithm follows by performing the learning update in the steepest descent direction:

$$u_{j+1} = u_j - \varepsilon \left. \frac{\partial \mathcal{J}(u_{j+1})}{\partial u_{j+1}} \right|_{u_{j+1}=u_j} = u_j + \varepsilon J^T W_e e_j - \varepsilon W_f u_j,$$

where the factor 2 is absorbed in the step size ε . \square

The upper bound $\bar{\varepsilon}$ on the learning gain ε is developed later, see Theorem 8 in Section III-D. In the following, it is shown that J^T has the interpretation of the adjoint operator of J .

Definition 3 (Adjoint). *Let the inner product of two signals be given by: $\langle u, g \rangle = u^T g$, with $u, g \in \mathbb{R}^N$. Then, for a linear operator J , the adjoint J^* is defined as the operator that satisfies the condition [33, Section 22]:*

$$\langle f, Jg \rangle = \langle J^* f, g \rangle \forall f, g \in \mathbb{R}^N.$$

Lemma 4 (Adjoint operator). *The adjoint J^* of operator J , see (2), is given by $J^* = J^T$.*

Proof. According to Definition 3, for a system J with adjoint J^* and signals $u_1, u_2 \in \mathbb{R}^N$, the following must hold:

$$u_1^T J u_2 = (J^* u_1)^T u_2 = u_1^T (J^*)^T u_2$$

From the above follows directly that for system J the adjoint $J^* = J^T$. \square

Thus, Lemma 4 reveals that the gradient descent ILC algorithm (5) can be interpreted as an adjoint-based algorithm.

C. Data-driven learning using the adjoint system

As will be shown, an operation with the adjoint of a linear time invariant SISO system can be recast to an operation on the original system and time-reversal of the in- and output signals. There are many applications that exploit this property, e.g., system identification [22], [23], [30], [24, Section 12.2] and iterative learning control [21, Section 36.3.3.1], [27], [28].

The time-reversal approach only applies to SISO systems. Indeed, as is shown next, the generalization to MIMO systems requires significantly more steps. The theory developed here exploits recent developments in system identification [30].

Before presenting the main results for MIMO systems, note that for a SISO system J^{11} , the adjoint J^{11T} can be recast to:

$$J^{11T} = \mathcal{R} J^{11} \mathcal{R} \quad (6)$$

with

$$\mathcal{R} = \begin{bmatrix} 0 & \cdots & 0 & 0 & 1 \\ 0 & \cdots & 0 & 1 & 0 \\ \vdots & & \ddots & 0 & 0 \\ 0 & \ddots & & \vdots & \vdots \\ 1 & 0 & \cdots & 0 & 0 \end{bmatrix}$$

an involutory permutation matrix with size $N \times N$. Here, \mathcal{R}_N is interpreted as a time-reversal operator. Consider the following operation:

$$y = J^{11T} u = \mathcal{R} J^{11} \mathcal{R} u. \quad (7)$$

It shows that the operation $y = J^{11T} u$ can be recast to an operation on the original system J^{11} , and time-reversing the input before applying operator J^{11} , and time-reversing the resulting output afterwards. Note that (6) is only valid for SISO systems and is exactly the same operation as is performed using the “FiltFilt” operation in Q -filtering [21, Section 36.3.3.1]. For a MIMO system J , the adjoint J^T can be written as:

$$J^T = \underbrace{\begin{bmatrix} \mathcal{R} & 0 \\ \ddots & \\ 0 & \mathcal{R} \end{bmatrix}}_{\mathcal{R}_{n_i}} \underbrace{\begin{bmatrix} J^{11} & \cdots & J^{n_o,1} \\ \vdots & & \vdots \\ J^{1,n_i} & \cdots & J^{n_o,n_i} \end{bmatrix}}_{\tilde{J}} \underbrace{\begin{bmatrix} \mathcal{R} & 0 \\ & \ddots \\ 0 & \mathcal{R} \end{bmatrix}}_{\mathcal{R}_{n_o}}, \quad (8)$$

here $\tilde{J} \in \mathbb{R}^{n_i N \times n_o N}$, and $\mathcal{R}_{n_i} \in \mathbb{R}^{n_i N \times n_i N}$, $\mathcal{R}_{n_o} \in \mathbb{R}^{n_o N \times n_o N}$ are time-reversal operators for the higher dimensional in- and output signals. Matrix \tilde{J} is the finite-time representation of $\tilde{J}(z) \in \mathbb{C}^{n_i \times n_o}$, with

$$\tilde{J}(z) = \begin{bmatrix} J^{11}(z) & \cdots & J^{n_o,1}(z) \\ \vdots & & \vdots \\ J^{1,n_i}(z) & \cdots & J^{n_o,n_i}(z) \end{bmatrix}.$$

If J a symmetric system then $\tilde{J} = J$, in this case (6) is valid and the SISO time-reversal approach in (7) can be applied. For general MIMO systems $\tilde{J} \neq J$.

The main idea of the presented approach is to develop a data-driven MIMO ILC algorithm by recasting the system $\tilde{J}(z)$ to:

$$\tilde{J}(z) = \sum_{i=1}^{n_i} \sum_{j=1}^{n_o} I^{ij} J(z) I^{ij}, \quad (9)$$

where $I^{ij} \in \mathbb{R}^{n_i \times n_o}$, is a static system with n_i outputs and n_o inputs. For the k^{th} and l^{th} entry of I^{ij} holds

$$\begin{aligned} I_{k=i,l=j}^{ij} &= 1, \\ I_{k \neq i, l \neq j}^{ij} &= 0, \end{aligned} \quad (10)$$

i.e., all entries are of I^{ij} zero, except the i^{th}, j^{th} entry. The structure of I^{ij} is given by

$$I^{ij} = \begin{bmatrix} 0^{i-1 \times j-1} & 0^{i-1 \times 1} & 0^{i-1 \times n_o-j} \\ 0^1 \times j-1 & 1 & 0^1 \times n_o-j \\ 0^{n_i-i \times j-1} & 0^{n_i-i \times 1} & 0^{n_i-i \times n_o-j} \end{bmatrix},$$

where $0^{i \times j}$ is the zero matrix with $\dim(0^{i \times j}) = (i, j)$. The role of I^{ij} in $\mathbf{y}(z) = \mathbf{J}(z) \mathbf{I}^{ij} \mathbf{u}(z)$ is selecting the j^{th} entry

in $\mathbf{u}(z)$ and apply it to the i^{th} input of $\mathbf{J}(z)$, where the rest of the inputs to $\mathbf{J}(z)$ are zero.

Let I^{ij} be the finite-time representation of I^{ij} , then the finite-time representation of \tilde{J} , see (9), is given by

$$\tilde{J} = \sum_{i=1}^{n_i} \sum_{j=1}^{n_o} I^{ij} J I^{ij}.$$

Substitution of the above in (8) yields the main result:

$$J^T = \mathcal{R}_{n_i} \left(\sum_{i=1}^{n_i} \sum_{j=1}^{n_o} I^{ij} J I^{ij} \right) \mathcal{R}_{n_o} \quad (11)$$

The above equation recasts the evaluation of J^T as $n_i \cdot n_o$ experiments on J . This approach is used with ILC algorithm (5), to arrive at the data-driven ILC algorithm for MIMO systems.

The following procedure provides the learning update for the ILC algorithm in Theorem 2.

Procedure 5 (Dedicated gradient experiment). *The objective is to compute $J^T e_j$ by performing experiments on J . This is achieved by applying the following sequence of steps:*

- 1) Time reverse $\bar{e}_j = \mathcal{R}_{n_o} e_j$
- 2) Compute \bar{z}_j by performing $n_i \cdot n_o$ experiments on J :

$$\bar{z}_j = \sum_{i=1}^{n_i} \sum_{j=1}^{n_o} I^{ij} J I^{ij} \bar{e}_j,$$

with I^{ij} the matrix representation of static system I_{ij} defined in (10).

- 3) Time reverse again to compute $J^T e_j = \mathcal{R}_{n_i} \bar{z}_j$

The main idea is to replace the model by dedicated experiments on the system. The above approach is visualized in a diagram for $n_i = n_o = 2$ in Fig. 2. The complete adjoint-based ILC algorithm (5) using the data-based learning update in (11) is summarized as follows.

Summary 6 (Data-driven ILC algorithm for MIMO systems). *Given an initial input u_0 , set $j = 0$, perform the following steps:*

- 1) execute a trial and measure $e_j = r - Ju_j$,
- 2) use Procedure 5 to experimentally determine $J^T W_e e_j$,
- 3) apply ILC algorithm (5), set $u_{j+1} = (I - \varepsilon W_f) u_j + \varepsilon J^T W_e e_j$,
- 4) set $j := j + 1$ and go back to step 1 or stop if a suitable stopping criterion is met.

Note that the inclusion of weighting matrix W_e in step 2 of Summary 6 is a straight-forward multiplication of e_j prior to using Procedure 11.

Remark 1. *All measured signals contain noise. In principle, to show that Procedure 5 yields unbiased results requires computing the expected value of the filtered e_j . A full stochastic proof that $J^T e_j$ resulting from Procedure 5 is indeed unbiased is outside the scope of this paper but follows along the lines of [34].*

Remark 2. *In this paper the steepest descent algorithm is used to optimize (4). The approach presented in this section*

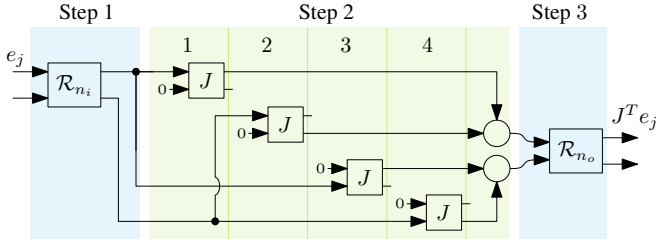


Fig. 2. Overview of Procedure 5 for $n_i = n_o = 2$.

is in principle directly applicable to any other optimization algorithm that uses first order gradient information. The data-based approach can also be extended to second order methods, as long as the optimization step is affine in the first and second order gradient. The second order gradient of (4) is given by

$$\frac{\partial^2 J(u_{j+1})}{\partial u_{j+1}^2} = 2J^T W_e J + 2W_f.$$

This expression can also be determined by performing experiments on J . Note that if e_j contains measurement noise, a direct estimate of $J^T W_e J e_j$ is biased, see [35] for unbiased estimates.

D. Convergence criteria

Firstly, monotonic convergence is given in Definition 7, secondly, the conditions for achieving monotonic convergence of ILC algorithm (5) are presented in Theorem 8.

Definition 7 (Monotonic convergence). *The ILC algorithm is monotonically convergent if and only if the following condition holds:*

$$\|u_{j+1} - u_\infty\| < \gamma \|u_j - u_\infty\|, \quad \forall u_j, u_{j+1} \quad (12)$$

with u_∞ the unique fixed point of iterative algorithm (5), the norm $\|\cdot\|$ as defined in Section III-A, and $\gamma \in [0, 1)$ a convergence rate.

See [1] and [10] for equivalent definitions.

Theorem 8 (Criterion for monotonic convergence). *Given weighting matrices $W_e > 0, W_f \geq 0$, such that and $J^T W_e J + W_f$ has full rank. Let $0 < \varepsilon \leq \bar{\varepsilon}$, then $\exists \bar{\varepsilon} > 0$ such that ILC algorithm (5) is monotonically convergent with*

$$\bar{\varepsilon} = 2\|J^T W_e J + W_f\|^{-1},$$

and converged signals

$$\begin{aligned} u_\infty &= \lim_{j \rightarrow \infty} u_j = (J^T W_e J + W_f)^{-1} J^T W_e r, \\ e_\infty &= \lim_{j \rightarrow \infty} e_j = (I - J(J^T W_e J + W_f)^{-1} J^T W_e) r. \end{aligned}$$

Proof. The proof is based on the contraction mapping theorem, see [33, Theorem 3.15.2]. The ILC trial dynamics can be recast to

$$\begin{aligned} u_{j+1} &= (I - \varepsilon W_f) u_j + \varepsilon J^T W_e e_j \\ &= (I - \varepsilon W_f) u_j + \varepsilon J^T W_e (r - J u_j) \\ &= (I - \varepsilon (J^T W_e J + W_f)) u_j + \varepsilon J^T W_e r. \end{aligned} \quad (13)$$



Fig. 3. Océ Arizona 550GT flatbed printer experimental setup. The printer is normally used to print on rigid media with applications in interior decoration, product decoration, signage, and art.

Let $M = I - \varepsilon(J^T W_e J + W_f)$, then, it can be verified that for the condition for monotonic convergence in Definition 7 holds

$$\|u_{j+1} - u_\infty\| - \|u_j - u_\infty\| = \|M u_j - M u_\infty\| - \|u_j - u_\infty\|.$$

Next, using $\|M u_j - M u_\infty\| \leq \|M\| \|u_j - u_\infty\|$ to bound $\|M u_j - M u_\infty\|$ from above it follows that if $\|M\| < 1$ then condition (12) for monotonic convergence is satisfied with $\gamma = \|M\|$.

Following similar lines as in [28] and [16] it follows that $\exists \varepsilon$ s.t. $\varepsilon < \bar{\varepsilon} \Rightarrow \|I - \varepsilon(J^T W_e J + W_f)\| < 1$ with $\bar{\varepsilon} = 2\|J^T W_e J + W_f\|^{-1}$ since $J^T W_e J + W_f$ has full rank.

If $\|M\| < 1$, then M is a contraction and the ILC algorithm in (5) converges to a unique fixed point u_∞ . The latter follows by setting $u_{j+1} = u_j = u_\infty$ in (13) and solving for u_∞ . Substitution of u_∞ in (3) yields e_∞ . \square

Remark 3. *Model-based gradient-descent algorithms require additional robustness considerations. In [16] the robustness properties of (model-based) gradient-descent ILC for SISO systems are investigated. Essentially, ε determines a trade-off between convergence rate and robustness for model uncertainty. For large modeling errors $\varepsilon \ll \bar{\varepsilon}$, with very slow convergence as a consequence. A common approach in improving convergence speed of algorithm (5) is using a trial-dependent ε_j , see e.g., [16, Section 8]. Extending the results to include such a ε_j is part of ongoing research.*

IV. SIMULATION RESULTS

The data-driven ILC approach for MIMO systems that is developed in Section III is simulated using a model of an industrial flatbed printer as system. The model is a high-fidelity 44th order state-space model that has been identified on the true system using experiments.

The flatbed printer is shown in Fig. 3 and an overview is presented in Fig. 4. The system has four degrees of freedom: the carriage has translations y and z , the gantry has a translation x , and a rotation φ which is defined around the point p_1 that is fixed to the center of the gantry.

1) *System:* The subsystem of the Arizona that is considered for control is the gantry. The gantry is controlled in x and φ direction using force actuators u_1 and u_2 , see Fig. 4.

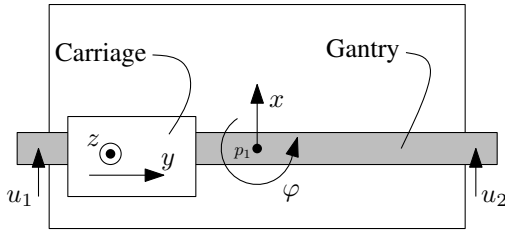


Fig. 4. Overview of the Arizona Setup. The printer has four motion axes: z and y translations for the carriage, the gantry translates in x direction and the rotation is φ . The gantry is considered for control in the present paper.

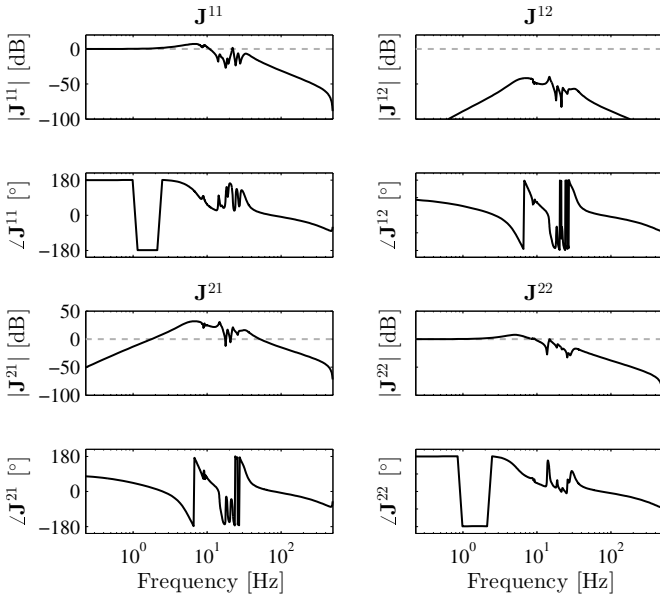


Fig. 5. Bode diagram of the closed-loop system $J(z)$.

The system operates in closed-loop with a given diagonal controller, hence system J , see Fig. 1, represents the feedback controlled system $y = Ju$, with:

$$y = \begin{bmatrix} x \\ \varphi \end{bmatrix}, \quad u = \begin{bmatrix} r_x \\ r_\varphi \end{bmatrix},$$

with r_x the reference for x and r_φ the reference for φ . A model of J has been identified using frequency response measurements. The Bode diagram corresponding to $J(z)$ is presented in Fig. 5. Analysis of the Bode diagram reveals that interaction deteriorates performance for frequencies of 2 Hz and above. This is caused by the large $|J^{21}|$, hence r_x has a large influence in φ . It is therefore expected that MIMO ILC can achieve a significant performance improvement.

The references for the gantry are presented in Fig. 6. The reference r_x is a smooth step of 40 mm and the reference r_φ represents a forth and back rotation of the gantry.

2) *ILC design*: To satisfy the condition for monotonic convergence in Theorem 8, the learning gain $\varepsilon = 0.95\bar{\varepsilon} = 0.0013$, with $\bar{\varepsilon} = 2\|JJ^TW_e\|^{-1}$. The weighting matrix $W_f = 0$ and W_e is a diagonal matrix $W_e = \text{diag}(w_{ex}I, w_{e\varphi}I)$ that is used to compensate for the different units of x and φ .

3) *Results*: The simulation is invoked with initial input $u_0 = [r_x, r_\varphi]^T$, hence the first trial hence corresponds

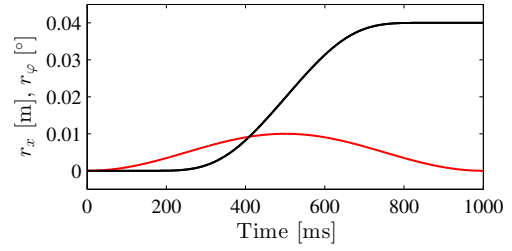


Fig. 6. References: r_x (black solid) is a 40 mm smooth step, r_φ (red solid) a forth and back rotation.

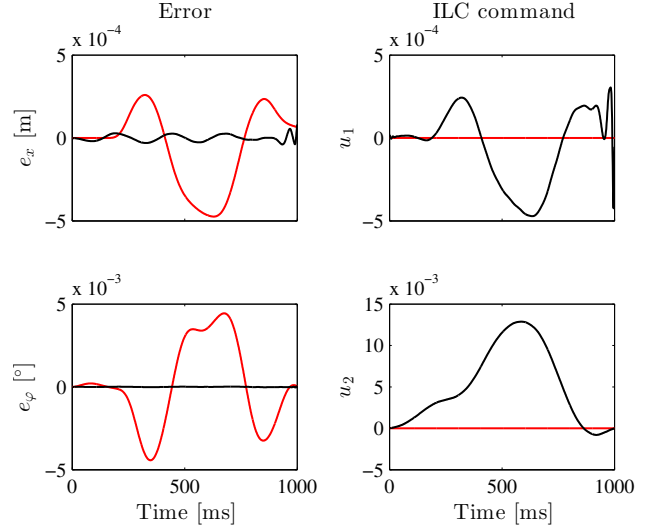


Fig. 7. Simulation results: tracking errors (left), ILC command signals (right). Feedback only (red solid), ILC (black solid). The results show a significant performance improvement in both e_x and e_φ when ILC is applied.

to the performance of the system with feedback control only. Sufficiently many trials for convergence are performed (5000) using the steps in Summary 6. The time domain tracking errors and resulting command signals are presented in Fig. 7. The results show that both e_x and e_φ have reduced significantly. The reduction in e_φ is larger, this is attributed to the fact that the large initial value of e_φ with feedback only is much larger than the initial value e_x , therefore the reduction of e_φ is emphasized more in the cost function. The cost function \mathcal{J} has reduced from $\mathcal{J}(u_0) = 6.65 \cdot 10^{-3}$ to $\mathcal{J}(u_{5000}) = 1.18 \cdot 10^{-6}$.

The results show a significant performance improvement using the presented ILC algorithm that does not require a model of the system in the learning update. The simulations hence show promising results for the ongoing work towards experiments on the Arizona setup.

V. CONCLUSIONS AND ONGOING RESEARCH

In this paper adjoint-based ILC algorithm for multivariable systems is presented. The approach is data-driven in the sense that it does not require a model for constructing the commonly used L and Q filters.

The main results show that the learning update with the adjoint system can be recast to performing multiple experiments on the original system. Convergence criteria

are developed. The results are supported with a simulation of an industrial multi-axis flatbed printer.

Currently, the presented algorithm is being implemented in an experiment. Subjects of ongoing research include: signal conditioning in the experiments, using basis functions for increased convergence speed and robustness against measurement noise [5], reducing the number of experiments needed in the data-driven approach, and an automated method for the selection of ε using the approach in [30].

ACKNOWLEDGMENT

The contributions of Stephan Kleinendorst are gratefully acknowledged. The authors would also like to acknowledge the fruitful discussions with the late professor Okko Bosgra, professor Maarten Steinbuch, and Sjirk Koekebakker.

This work is supported by Océ Technologies, P.O. Box 101, 5900 MA Venlo, The Netherlands. This work is also supported by the Innovational Research Incentives Scheme under the VENI grant “Precision Motion: Beyond the Nanometer” (no. 13073) awarded by NWO (The Netherlands Organisation for Scientific Research) and STW (Dutch Science Foundation).

REFERENCES

- [1] D. Bristow, M. Tharayil, and A. Alleyne, “A Survey of Iterative Learning Control: a Learning-based Method for High-performance Tracking Control,” *IEEE Control Systems Magazine*, vol. 26, pp. 96–114, 2006.
- [2] K. Barton, D. Hoelzle, A. Alleyne, and A. Johnson, “Cross-Coupled Iterative Learning Control of Systems with Dissimilar Dynamics: Design and Implementation for Manufacturing Applications,” *International Journal of Control*, vol. 84, pp. 1223–1233, 2011.
- [3] D. Hoelzle, A. Alleyne, and A. Johnson, “Basis Task Approach to Iterative Learning Control With Applications to Micro-Robotic Deposition,” *IEEE Transactions on Control Systems Technology*, vol. 19, pp. 1138–1148, 2011.
- [4] J. Wallén, M. Norrlöf, and S. Gunnarsson, “A Framework for Analysis of Observer-based ILC,” *Asian Journal of Control*, vol. 13, pp. 3–14, 2011.
- [5] J. Bolder, T. Oomen, S. Koekebakker, and M. Steinbuch, “Using Iterative Learning Control with Basis Functions to Compensate Medium Deformation in a Wide-format Inkjet Printer,” *Mechatronics*, vol. 24, pp. 944–953, 2014.
- [6] S. Mishra, J. Coaplen, and M. Tomizuka, “Precision Positioning of Wafer Scanners Segmented Iterative Learning Control for Nonrepetitive Disturbances,” *IEEE Control Systems Magazine*, vol. 27, pp. 20–25, 2007.
- [7] S. van der Meulen, R. Tousain, and O. Bosgra, “Fixed Structure Feedforward Controller Design Exploiting Iterative Trials: Application to a Wafer Stage and a Desktop Printer,” *Journal of Dynamic Systems, Measurements, and Control: Transactions of the ASME*, vol. 130, pp. 1–16, 2008.
- [8] M. Heertjes, D. Hennekens, and M. Steinbuch, “MIMO Feed-forward Design in Wafer Scanners Using a Gradient Approximation-based Algorithm,” *Control Engineering Practice*, vol. 18, pp. 495–506, 2010.
- [9] R. Longman, “Iterative Learning Control and Repetitive Control for Engineering Practice,” *International Journal of Control*, vol. 73, pp. 930–954, 2000.
- [10] M. Norrlöf and S. Gunnarsson, “Time and Frequency Domain Convergence Properties in Iterative Learning Control,” *International Journal of Control*, vol. 75, pp. 1114–1126, 2002.
- [11] N. Amann, D. Owens, and E. Rogers, “Iterative Learning Control Using Optimal Feedback and Feedforward Actions,” *International Journal of Control*, vol. 65, pp. 277–293, 1996.
- [12] J. Lee, K. Lee, and W. Kim, “Model-based Iterative Learning Control with a Quadratic Criterion for Time-varying Linear Systems,” *Automatica*, vol. 36, pp. 641–657, 2000.
- [13] S. Gunnarsson and M. Norrlöf, “On the design of ILC algorithms using optimization,” *Automatica*, vol. 37, pp. 2011–2016, 2001.
- [14] K. Kinoshita, T. Sogo, and N. Adachi, “Iterative Learning Control Using Adjoint Systems and Stable Inversion,” *Asian Journal of Control*, vol. 1, pp. 60–67, 2002.
- [15] J. Ratcliffe, J. Hätönen, P. Lewin, E. Rogers, and D. Owens, “Robustness Analysis of an Adjoint Optimal Iterative Learning Controller with Experimental Verification,” *International Journal of Robust and Nonlinear Control*, vol. 18, pp. 1089–1113, 2008.
- [16] D. Owens, J. Hätönen, and S. Daley, “Robust Monotone Gradient-based Discrete-time Iterative Learning Control,” *International Journal of Robust and Nonlinear Control*, vol. 19, pp. 634–661, 2009.
- [17] T. Son, G. Pipeleers, and J. Swevers, “Experimental Validation of Robust Iterative Learning Control on an Overhead Crane Test Setup,” *IFAC Triennial World Congress, Cape Town, South Africa*, pp. 5981–5986, 2014.
- [18] J. van de Wijdeven, M. Donkers, and O. Bosgra, “Iterative Learning Control For Uncertain Systems: Noncausal Finite Time Interval Robust Control Design,” *International Journal of Robust and Nonlinear Control*, vol. 21, pp. 1645–1666, 2011.
- [19] D. Bristow and A. Alleyne, “Monotonic Convergence of Iterative Learning Control for Uncertain Systems Using a Time-varying Filter,” *IEEE Transactions on Automatic Control*, vol. 53, pp. 582–585, 2008.
- [20] A. Tayebi and M. Zaremba, “Robust Iterative Learning Control Design is Straightforward for Uncertain LTI Systems Satisfying the Robust Performance Condition,” *IEEE Transactions on Automatic Control*, vol. 48, pp. 101–106, 2003.
- [21] D. Bristow, K. Barton, and A. Alleyne, *Iterative Learning Control, Chapter 36 in the Control Systems Handbook - Second Edition*, W. S. Levine, Ed. CRC Press, Taylor & Francis Group, 2011.
- [22] C. Rojas, T. Oomen, H. Hjalmarsson, and B. Wahlberg, “Analyzing Iterations in Identification With Application to Nonparametric \mathcal{H}_∞ -norm Estimation,” *Automatica*, vol. 48, pp. 2776–2790, 2012.
- [23] B. Wahlberg, M. Syberg, and H. Hjalmarsson, “Non-parametric Methods for \mathcal{L}_2 -gain Estimation Using Iterative Experiments,” *Automatica*, vol. 46, pp. 1376–1381, 2010.
- [24] H. Hjalmarsson, “From Experiment Design to Closed-loop Control,” *Automatica*, vol. 41, pp. 393–438, 2005.
- [25] B. Potsaid and J. Wen, “High Performance Motion Tracking Control,” *Proceedings of the Conference on Control Applications, Taipei, Taiwan*, pp. 719–723, 2004.
- [26] Y. Ye and D. Wang, “Zero Phase learning Control Using Reversed Time Input Runs,” *Journal of Guidance, Control, and Dynamics*, vol. 127, pp. 133–139, 2005.
- [27] C. Freeman, P. Lewin, and E. Rogers, “Further Results on the Experimental Evaluation of Iterative Learning Control Algorithms for Non-minimum Phase Plants,” *International Journal of Control*, vol. 80, pp. 569–582, 2007.
- [28] M. Butcher, A. Karimi, and R. Longchamp, “Iterative Learning Control based on Stochastic Approximation,” *IFAC Triennial World Congress*, vol. 17, pp. 1478–1483, 2008.
- [29] M.-B. Rădac, R.-E. Precup, E. Petriu, S. Preitl, and C.-A. Dragoș, “Data-Driven Reference Trajectory Tracking Algorithm and Experimental Validation,” *IEEE Transactions on Industrial Informatics*, vol. 9, pp. 2327–2336, 2013.
- [30] T. Oomen, R. van der Maas, C. Rojas, and H. Hjalmarsson, “Iterative Data-Driven \mathcal{H}_∞ Norm Estimation of Multivariable Systems With Application to Robust Active Vibration Isolation,” *IEEE Transactions on Control Systems Technology*, vol. 22, pp. 2247–2260, 2014.
- [31] Z.-S. Hou and Z. Wang, “From Model-based Control to Data-driven Control: Survey, Classification and Perspective,” *Information Sciences*, vol. 235, pp. 3–35, 2013.
- [32] R. Chia, D. Wang, Z. Hou, and S. Jin, “Data-driven Optimal Terminal Iterative Learning Control,” *Journal of Process Control*, vol. 22, pp. 2026–2037, 2012.
- [33] A. Naylor and G. Sell, *Linear Operator Theory in Engineering and Science*. Springer, 1982.
- [34] H. Hjalmarsson, M. Gevers, S. Gunnarsson, and O. Lequin, “Iterative Feedback Tuning: Theory and Applications,” *IEEE Control Systems*, vol. 18, pp. 26–41, 1998.
- [35] G. Solari and M. Gevers, “Unbiased estimation of the Hessian for iterative feedback tuning,” *Proceedings of the Conference on Decision and Control, Paradise Island, Bahamas*, pp. 1759–1760, 2004.